SoftwareX 23 (2023) 101405

Contents lists available at ScienceDirect

SoftwareX

journal homepage: www.elsevier.com/locate/softx

Original software publication

MaranStable: A linear stability solver for multiphase flows in canonical geometries

Mario Stojanović [a,*], Francesco Romanò [b], Hendrik C. Kuhlmann [a]

[a] TU Wien, Getreidemarkt 9-BA, 1060 Vienna, Austria

[b] Univ. Lille, CNRS, ONERA, Arts et Métiers Institute of Technology, Centrale Lille, UMR 9014 – LMFL – Laboratoire de Mécanique des Fluides de Lille – Kampé de Fériet, F-59000 Lille, France

ARTICLE INFO

Article history:
Received 27 February 2023
Received in revised form 27 April 2023
Accepted 4 May 2023

Dataset link: https://github.com/fromano88/MaranStable.git

Keywords:
Navier–Stokes equations
Multiphase flow
GUI
Thermocapillary flow

ABSTRACT

MaranStable is a software to perform three-dimensional linear stability analyses of steady two-dimensional non-isothermal multiphase flows in canonical geometries. Different approximations to the Navier–Stokes equations can be selected, which are discretized by finite volumes on a staggered grid. The stability of the basic flow, obtained by Newton—Raphson iteration, is computed by solving the linearized three-dimensional perturbation equations using normal modes. All calculations are based on MATLAB and make extensive use of the already parallelized backslash and eigs operators, and the graphical user interface eases the access to MaranStable.

Code metadata

Current code version	3.1
Permanent link to code/repository used for this code version	https://github.com/ElsevierSoftwareX/SOFTX-D-23-00135
Permanent link to Reproducible Capsule	
Legal Code License	CC-BY-NC-SA
Code versioning system used	none
Software code languages, tools, and services used	MATLAB
Compilation requirements, operating environments & dependencies	MATLAB R2022a or newer; OS tested: Windows 10, Ubuntu 18.04.6
If available Link to developer documentation/manual	https://github.com/fromano88/MaranStable/tree/main/docs
Support email for questions	maranstable@tuwien.ac.at

Software metadata

Current software version	3.1
Permanent link to executables of this version	https://github.com/fromano88/MaranStable/tree/main/bin
Permanent link to Reproducible Capsule	
Legal Software License	CC-BY-NC-SA
Computing platforms/Operating Systems	OS tested: Windows 10, Ubuntu 18.04.6
Installation requirements & dependencies	MATLAB R2022a or newer
If available, link to user manual - if formally published include a reference to the publication in the reference list	https://github.com/fromano88/MaranStable/tree/main/docs
Support email for questions	maranstable@tuwien.ac.at

1. Motivation and significance

Flow instabilities occur everywhere. They change the structure of the flow in nature and in engineering applications. Three scenarios demonstrate the crucial importance of hydrodynamic

* Corresponding author.
E-mail address: mario.stojanovic@tuwien.ac.at (Mario Stojanović).

https://doi.org/10.1016/j.softx.2023.101405

instability for the system dynamics: (a) The capillary break-up of a liquid jet initiated by the Rayleigh instability is relevant to inkjet printing. (b) Shear-flow instabilities related to the laminar–turbulence transition significantly affect the drag forces. (c) Buoyancy-driven instabilities are largely employed in thermal management of buildings with floor heating or ceiling cooling and drive geophysical circulations. While the physical mechanisms changing the flow character by instability are different, they all derive from the nonlinear character of the Navier–Stokes equations.

`MaranStable` computes the parameters (e.g. the Reynolds number) at which the flow changes by instability. The code can deal with different canonical geometries (channels, annular pipes, cavities, etc.). It thus computes the essential instability phenomenon which might be hidden by excessive details in a comprehensive engineering model. For instance, the thermocapillary instabilities of the flow in a generic liquid bridge is the origin of striation imperfections in floating-zone crystal growth.

With this paper we make `MaranStable` publicly available and thus provide the mathematics, physics, and engineering communities with software capable of computing basic two-dimensional immiscible multiphase flows involving capillary and Marangoni stresses, and static and dynamic interface deformations. The solver can also compute the most dangerous mode and the critical parameter (e.g. the Reynolds number) beyond which the mode grows exponentially in time.

2. Software description

The governing equations are discretized by second-order finite volumes on a staggered grid. Primitive variables are used to solve the Navier–Stokes equations. Discrete pressure and temperature values are located at the cell centers, while the velocities are defined normal to and in centers of the cell faces which facilitates balancing the convective fluxes. The computational mesh is generated using a `MaranStable` tool capable of combining multiple tensorial grids (blocks), face-matched at their boundaries. Whenever curved boundaries are present, the solver body-fits the grid to the boundaries to avoid errors associated with geometric approximations at the order of accuracy of the discretization. For multiphase flows all blocks across the interface are body-fitted to the sharp interface. Thus the correct thermophysical properties are assigned to each phase with pressure and shear stress discontinuities across the interface due to capillary and Marangoni stresses, respectively. The curved interface location is solved either employing a static or a dynamic stress balance. Each block of the mesh is refined along its coordinate lines either by hyperbolic tangent or geometric progression, controlled by specifying the maximum and minimum grid sizes in each tensorial direction.

The basic flow state is an equilibrium solution of the steady two-dimensional Navier–Stokes equations. It is computed by the Newton–Raphson method using the MATLAB operator `backslash` which requires a good initial guess. A computed basic state can serve as an initial guess for consecutive basic state computations in the sense of a natural continuation. Once the sought basic state is obtained, its stability is computed from the linearized equations governing small perturbations. These are represented by Fourier modes in the homogeneous spatial direction (spanwise or azimuthal) and by an exponential behavior in time. This ansatz yields a generalized eigenvalue problem for the complex growth rate (eigenvalue) and the spatial structure of the perturbation flow (eigenvector). The eigenvalue problem is solved using the MATLAB operator `eigs`, which relies on the functions implemented in the ARPACK library [1] for linear algebra, and a Cayley transform implemented in `MaranStable`. `MaranStable` either returns the normalized perturbation flow of the *most dangerous mode* together with its growth rate and frequency at the given set of parameters or seeks the *critical mode* whose growth rate vanishes at a particular value of the control parameter. The user can opt to either search for the most dangerous or the critical mode. The latter is found by an automatic variation of one of the controlling parameters which is stepwise ramped up or down until the sign of the growth rate changes. The zero of the growth rate is then determined by a regula falsi [2] and the critical mode is obtained. More details on the mathematics, implementation and validation can be found in [3]. A corresponding simulation-resuming and parameter continuation algorithm is provided in `MaranStable` and is automatically called whenever required.

2.1. Software architecture

Running the script `main.m`, the GUI of `MaranStable` is launched and guides the user through all steps to set up a simulation. This same GUI is accessible by installing the executable for Windows or Linux and launching `MaranStable` by double clicking on the desktop icon without the need of installing MATLAB. The architecture of `MaranStable` is summarized in Fig. 1. Four macro-modules can be identified: (i) solver selection (green box in Fig. 1), (ii) initialization (blue boxes), (iii) simulation (red boxes), and (iv) visualization and post-processing (yellow boxes). A single- or a two-phase flow can be selected (i). During the initialization (ii), the user specifies the thermophysical properties of the fluids, the geometry, the parameters for the mesher, the approximation of the Navier–Stokes equations and the boundary conditions for the flow. Thereafter (iii), the simulation parameters shall be set, including the convergence criteria, the initial guess and the type of simulation (basic state, linear stability analysis, optical ray tracing). A comprehensive post-processing/visualization tool (iv) is included in the GUI. The data can be exported in VTK or DAT. The latter format is suitable for external line plotting. When a simulation is resumed, the macro-modules (ii) – (iv) work independently: Instead of going through (ii), the user can either load a previous initialization data set, a previously computed basic state, or a previously computed perturbation flow (see 'Load' button in Fig. 1). If the basic state has already been computed, the user can either skip (ii) and perform a stability analysis in (iii) or also skip (iii) and visualize the results in the macro-module (iv). The user may also change the parameters in (ii) and use the loaded flow field as an initial guess for a subsequent basic state computation. If the loaded file contains a computed perturbation flow, it can also be directly transferred to the post-processing (iv). Saving and resuming is done via the GUI, which grants high flexibility in the file naming. The resuming option is implemented only for states saved in `mat`-format.

2.2. Software capabilities

`MaranStable` provides the user with a highly flexible geometry set-up, of which only a few representative combinations are illustrated as examples in Fig. 2. However, we limit the solver to the case in which $\boldsymbol{g}$ is parallel to the axis of symmetry (symmetry plane) whenever gravitational forces are present. Regarding the governing equations, three versions of the continuity, Navier–Stokes, and energy equations are implemented in `MaranStable` for immiscible multiphase flows which are, with ascending complexity,

OB: **O**berbeck–**B**oussinesq approximation

$$\nabla \cdot \boldsymbol{u} = 0, \tag{1a}$$

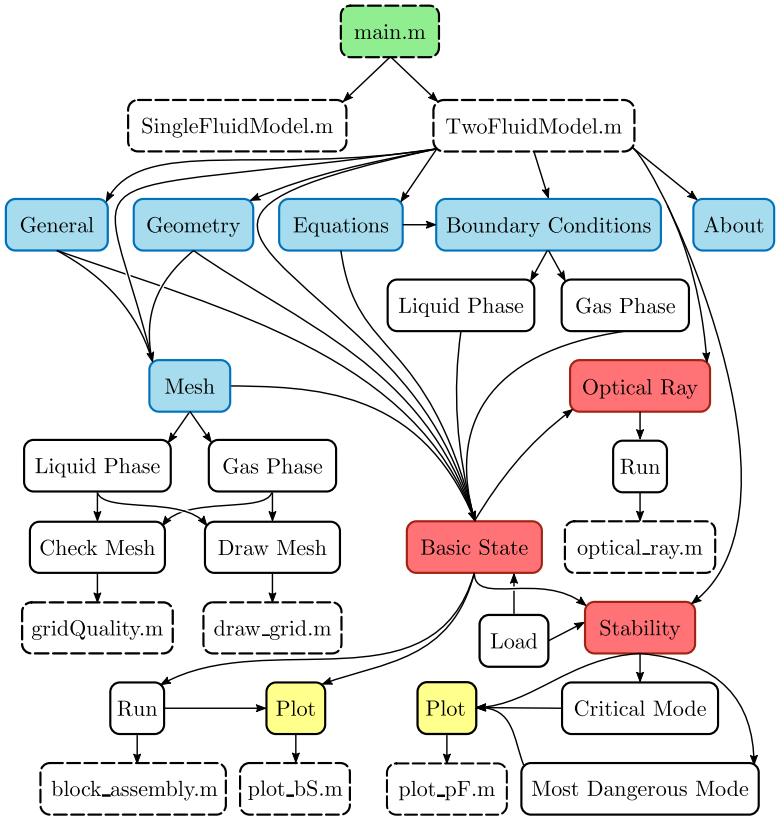

Fig. 1. Flowchart of `MaranStable`, only shown for the two-fluid model. For the single-fluid model, the flowchart is formally identical apart from the missing 'Gas Phase'. The four macro-modules are coded by color. Green: solver selection (i). Blue: initialization (ii). Red: simulation (iii). Yellow: visualization and post-processing (iv). Colored frames (blue and red) constitute the main tabs of the GUI. Black full frames indicate subordinated tabs or buttons. Black dashed frames represent source files.

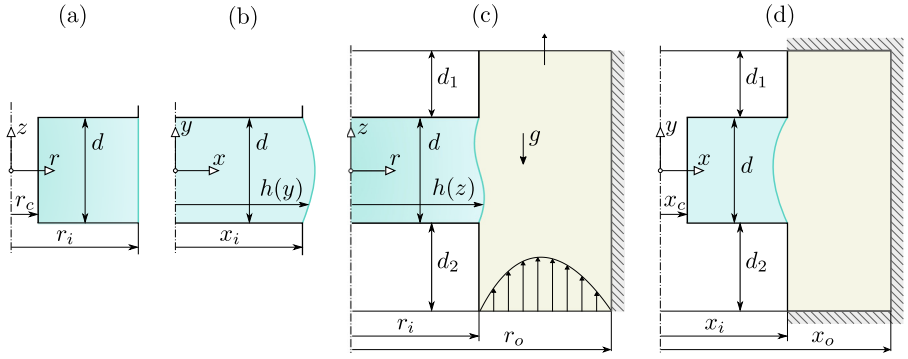

Fig. 2. Schematics of possible setups and coordinates: (a, c) cylindrical, (b, d) Cartesian. All geometrical parameters, as well as the volume ratio $\mathcal{V} = V_{\text{liquid}}/V_{\text{gap}}$, are adjustable, where V_{gap} is the upright gap between the two rods/blocks of radius r_i (or blocks of width x_i). Light blue: liquid phase. Beige: gas phase. (a, b): single-fluid model. (c, d): two-fluid model.

$$\partial_t \boldsymbol{u} + \boldsymbol{u}\cdot\nabla\boldsymbol{u} = -\frac{1}{\rho_{0i}}\nabla p + \frac{\mu_{0i}}{\rho_{0i}}\nabla^2\boldsymbol{u} - \boldsymbol{g}\alpha_{\rho i}(T - T_0), \tag{1b}$$

$$\partial_t T + \boldsymbol{u}\cdot\nabla T = \frac{\lambda_{0i}}{\rho_{0i}c_{p0i}}\nabla^2 T, \tag{1c}$$

LTD: **L**inearly **T**emperature-**D**ependent properties

$$-\rho_{0i}\alpha_{\rho i}\partial_t T + \nabla\cdot(\rho_i\boldsymbol{u}) = 0, \tag{2a}$$

$$\rho_i\left(\partial_t\boldsymbol{u} + \boldsymbol{u}\cdot\nabla\boldsymbol{u}\right) = -\nabla p + \nabla\cdot(\mu_i\boldsymbol{\tau}) - \boldsymbol{g}\alpha_{\rho i}(T - T_0), \tag{2b}$$

$$\rho_i c_{pi}\left(\partial_t T + \boldsymbol{u}\cdot\nabla T\right) = \lambda_i\nabla^2 T + \lambda_{0i}\alpha_{\lambda i}\left(\nabla T\right)^2, \tag{2c}$$

FTD: **F**ully **T**emperature-**D**ependent properties

$$\partial_t\rho_i + \nabla\cdot(\rho_i\boldsymbol{u}) = 0, \tag{3a}$$

$$\partial_t(\rho_i\boldsymbol{u}) + \nabla\cdot(\rho_i\boldsymbol{u}\boldsymbol{u}) = -\nabla p + \nabla\cdot(\mu_i\boldsymbol{\tau}) + \rho_i\boldsymbol{g}, \tag{3b}$$

$$\partial_t(\rho_i c_{pi}T) + \nabla\cdot(\rho_i c_{pi}T\boldsymbol{u}) = \nabla\cdot(\lambda_i\nabla T), \tag{3c}$$

where the index $i = 1, 2$ denotes the phase (only for the two-fluid model), t is the time, $\boldsymbol{u}$, p and T denote the velocity, pressure and temperature fields, $\boldsymbol{\tau} = \nabla\boldsymbol{u} + (\nabla\boldsymbol{u})^{\mathrm{T}} - 2(\nabla\cdot\boldsymbol{u})\mathcal{I}/3$ and $\mathcal{I}$ are (twice) the deformation rate tensor and the identity matrix, respectively. The thermo-physical properties ρ, μ, c_p and λ are the temperature-dependent density, dynamic viscosity, specific heat at constant pressure and thermal conductivity, respectively.

The physical model among OB, LTD and FTD is selected in the macro-module (ii) inside the main tab 'General'.

In the Boussinesq approximation OB all thermo-physical material parameters are assumed constant and evaluated at a reference temperature T_0 (subscript '0'), except for the linear dependence of the density in the buoyancy term. Within the LTD model, the material parameters

$$\mu_i = \mu_{0i}\left[1 - \alpha_{\mu i}(T - T_0)\right], \tag{4a}$$
$$\rho_i = \rho_{0i}\left[1 - \alpha_{\rho i}(T - T_0)\right], \tag{4b}$$
$$\lambda_i = \lambda_{0i}\left[1 + \alpha_{\lambda i}(T - T_0)\right], \tag{4c}$$
$$c_{pi} = c_{p0i}\left[1 + \alpha_{cpi}(T - T_0)\right], \tag{4d}$$

depend linearly on T, where $c_{p0}\alpha_{cp}$, $\lambda_0\alpha_\lambda$, $-\rho_0\alpha_\rho$ and $-\mu_0\alpha_\mu$ are the linear coefficients of the Taylor expansions about $T = T_0$. Finally, within the FTD model, the user can choose among various implemented fluids, whose material properties depend nonlinearly on T. When choosing the OB or the LTD model, the user has the possibility to create a new fluid with custom material properties.

At the interface between two fluids, the balance of tangential and normal stresses, as well as the heat transfer across the interface is imposed. The capillary and Marangoni stresses are included in the interfacial conditions. Concerning the location of the interface h, we neglect dynamic surface deformations due to the three-dimensional perturbation flow, i.e., the stationary surface shape h of the basic state is prescribed while solving the perturbation equations. In that case, the interface location h depends only on the vertical coordinate (y for Cartesian and z for cylindrical coordinates, see Fig. 2). Within this constraint, three approximations are implemented in `MaranStable` with ascending complexity which can be selected in the macro-module (ii) inside 'Boundary Conditions':

RI: Straight indeformable surface shape (**R**igid **I**nterface) and linearized surface tension σ

$$h \equiv \begin{cases} x_i & \text{for Cartesian coordinates,} \\ r_i & \text{for cylindrical coordinates,} \end{cases} \tag{5a}$$
$$\sigma = \sigma_0 - \gamma(T - T_0), \tag{5b}$$

SI: Indeformable hydrostatic surface shape (**S**tatic **I**nterface) (limit of asymptotically large surface tension at reference temperature σ_0) and linearized surface tension

$$\Delta p_h = \sigma_0 \nabla \cdot \boldsymbol{n} + \Delta\rho_h g z, \tag{6a}$$
$$\sigma = \sigma_0 - \gamma(T - T_0), \tag{6b}$$

DI: Dynamically deformed surface shape (**D**ynamic **I**nterface) and full temperature-dependent surface tension

$$\Delta p_h = \sigma \nabla \cdot \boldsymbol{n} + \Delta\rho_h g z + \mu_1 \boldsymbol{n} \cdot \tau_1 \cdot \boldsymbol{n} - \mu_2 \boldsymbol{n} \cdot \tau_2 \cdot \boldsymbol{n}, \tag{7a}$$
$$\sigma = \sigma(T). \tag{7b}$$

Here $\gamma = -\partial_T \sigma|_{T_0}$ is the negative surface tension coefficient evaluated at the reference temperature T_0, Δp_h the interfacial pressure jump, $\Delta\rho_h$ the interfacial density jump and $\boldsymbol{n} = \boldsymbol{n}(h)$ the unit normal vector directed from phase 1 to phase 2. Selecting SI, the general stress balance on the interface (7a) reduces to the Young–Laplace Eq. (6a) which can be solved independently from the flow field [3]. However, in DI, the interface shape h is part of the numerical solution, since flow-induced deformations are taken into account in the basic state. This is taken care of by an additional iteration loop embedded in the Newton—Raphson iteration for the basic state.

A dedicated tab of the GUI guides the user through the boundary conditions. They can be chosen among: '`no-penetration`' (free-slip or no-slip boundary with either adiabatic conditions or a given temperature profile), '`free-surface`' (free-slip with user-specified heat flux, only for single-phase simulations) and '`outflow`' (constant-pressure with homogeneous Neumann conditions for velocity and temperature). Under the '`inflow`' conditions, the user can define a combination of non-homogeneous Dirichlet and homogeneous Neumann conditions allowing for case-specific inlet velocity and temperature profiles. Finally, `MaranStable` provides a module dedicated to optical ray tracing in axisymmetric, non-homogeneous diffraction index fields $\mathcal{N}$. This is coupled with the Navier–Stokes solver, as the user can provide a temperature-dependent $\mathcal{N}(T)$ index and trace the optical path in the liquid of a ray with normal incidence on a (transparent) wall.

2.3. Visualization, post-processing and customization

Several visualization and data post-processing features are implemented in `MaranStable`. The GUI provides a dedicated button for a post-processing of the data (velocity, pressure, and temperature fields) and visualization of the two-dimensional basic state and the three-dimensional critical mode. The computation of the Stokes stream function is implemented for planar and axisymmetric basic states. Beside of the embedded visualization toolbox, an export feature is available to save the flow in VTK and DAT formats. The exported data can be readily imported in third-party software for a more advanced graphical post-processing, like `ParaView` (VTK) or, for line graphs, `gnuplot`, `xmgrace`, etc. (DAT).

`MaranStable` can be further customized. One can switch from planar to axisymmetric geometries (Fig. 2). Moreover, by box-ticking one can select the physical model, activate/deactivate Marangoni stresses, use the creeping flow approximation (inertia terms in the OB, LTD and FTD models are set to zero) or skip the energy equation. Several fluids with their thermo-physical properties are already implemented in `MaranStable`. Additional fluids can be defined, but $\rho(T)$, $c_p(T)$, $\lambda(T)$, and $\mu(T)$ must either be constant or depend linearly on T. Fluids can also be defined as to enable a fully non-dimensional formulation, cf. Section 3.1.

3. Illustrative examples

3.1. Rayleigh-Bénard instability

In an infinitely extended layer of a Boussinesq fluid heated from below the conducting basic state becomes unstable due to buoyancy forces when a critical Rayleigh number is exceeded. To set up this problem, we use a single-fluid model governed by the OB model in a finite Cartesian domain with free-slip conditions on the horizontal top and bottom walls which are heated from below with a temperature difference ΔT. The domain (layer) has a thickness of $d = 1$ mm and the acceleration of gravity $\boldsymbol{g} = -g\boldsymbol{e}_y$ acts in the negative y direction. Since convection in plane layers arises in form of stationary periodic counter-rotating rolls with rectangular cross-section, periodic boundary conditions are equivalent, in this case, to adiabatic free-slip conditions on the cell boundaries. These conditions are thus imposed on the side walls of the present finite domain, whose length represents one wavelength $2\pi/k$ of the flow pattern, where k is the wave number in units of d^{-1}. The control parameter is the Rayleigh number $\mathrm{Ra} = g\alpha_\rho \Delta T d^3 \rho_0^2 c_{p0}/\mu_0\lambda_0$.

Neutral Rayleigh numbers Ra_n are defined by a vanishing growth rate. Results for Ra_n are shown in Fig. 3(a) as function of the wave number k. For the selected range of k, `MaranStable` (red crosses) reproduces the exact solution $\mathrm{Ra}_n^{\mathrm{exact}} = (k^2 + \pi^2)^3/k^2$ [4,5] (full line) up to 0.01% using a uniformly distributed

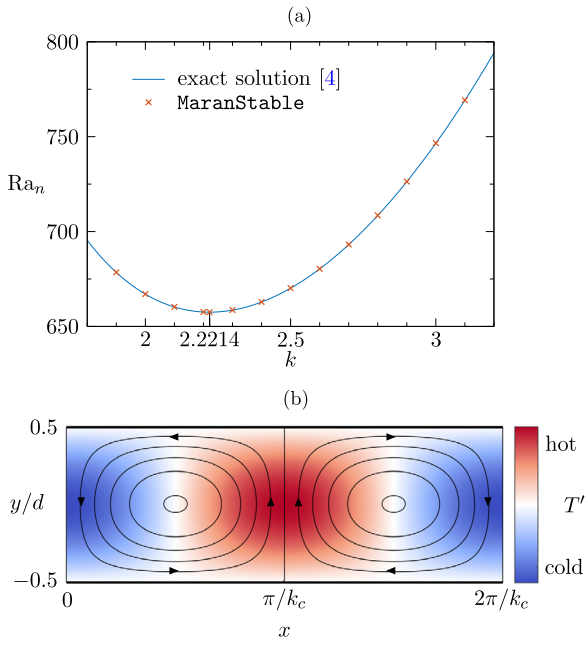

Fig. 3. (a) Neutral curve for the Rayleigh-Bénard problem with free-slip conditions at the top and bottom boundaries; crosses: `MaranStable`, line: exact solution. (b) Streamlines and temperature field T' (color) of the critical mode ($k = k_c = 2.2214$).

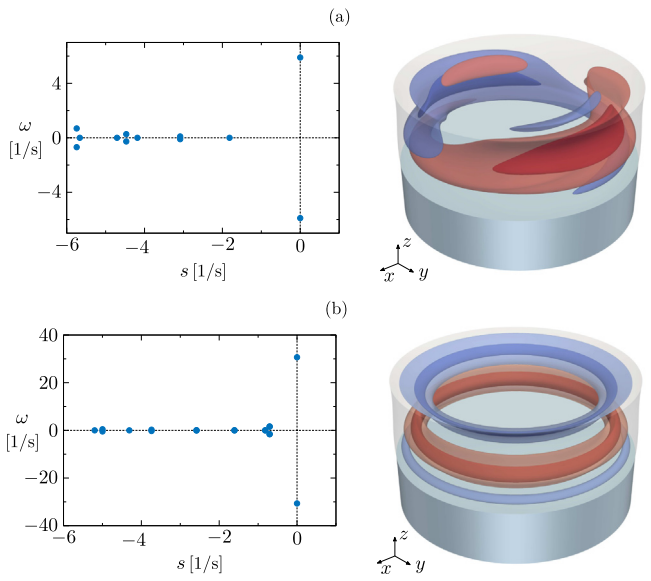

Fig. 4. Leading eigenvalues (left) and critical temperature field (right) for the same parameters, but different computational models. (a) Oberbeck–Boussinesq approximation OB with $m_c = 1$ and $\Delta T_c = 52.2$ °C. (b) Full temperature-dependent properties FTD with $m_c = 0$ and $\Delta T_c = 56.1$ °C.

grid with 28 300 grid points. The critical wave number k_c (minimum of Ra$_n$) found by `MaranStable` deviates by less than 10^{-4} % from $k_c^{\text{exact}} = \pi/\sqrt{2}$. The critical mode obtained by `MaranStable` is shown in Fig. 3(b).

3.2. Thermocapillary liquid bridge with a coaxial gas flow

An example for a multiphase problem with temperature-dependent fluid properties is the flow instability in an axisymmetric liquid bridge from silicone oil, which is treated using cylindrical coordinates. The liquid bridge is heated differentially with ΔT via cylindrical support rods and surrounded by air which is concentrically confined by a cylindrical tube. The basic flow is driven along the liquid–gas interface by the thermocapillary effect and by a steady forced nominally axial flow in the air. For more information, the reader is referred to [6].

Results of linear stability analyses are shown in Fig. 4. `MaranStable` can visualize the eigenvalue spectrum (left), where ω is the frequency and s the growth rate of the critical mode. The temperature field of one of the two oscillatory critical modes is shown on the right. Figures 4(a) and 4(b) are obtained for the same parameters, but for flow models OB and FTD, respectively, which yields different critical temperature differences ΔT_c. In both cases the critical mode is a wave, but it travels azimuthally with $m = 1$ for the OB model, while it is axisymmetric ($m = 0$) traveling axially for the FTD model.

3.3. Optical ray tracing

Finally, we demonstrate the ray tracing capability of `MaranStable`. The axisymmetric basic flow in a thermocapillary liquid bridge made from 2-cSt silicone oil with volume ratio $\mathcal{V} = 0.9$ and aspect ratio $\Gamma = d/r_i = 0.5$ is computed using the two-fluid model FTD for a temperature difference $\Delta T = 70$ °C ($T_0 = 25$ °C) under weightlessness. This corresponds to typical experimental conditions [8] for tracking particles in the liquid bridge through a transparent top rod. `MaranStable` can correct the hypothetical particle position (along the straight dashed line in Fig. 5) for a constant index of refraction $\mathcal{N}$ of the liquid to take into account the temperature dependence of $\mathcal{N}(T)$ (red line).

4. Impact and conclusions

`MaranStable` aims to provide the mathematics, physics and engineering community with a flexible and easy-to-use GUI-integrated code for performing linear stability analyses in immiscible multiphase flows.

The canonical geometries implemented in `MaranStable` cover many paradigmatic setups used to investigate flow instabilities. Examples were presented in Section 3. The range of Navier–Stokes (OB, LTD, FTD) and interfacial models (RI, SI, DI) implemented provides a large flexibility for carrying out state-of-the-art research in complex multiphase hydrodynamic stability. Several articles based on `MaranStable` have recently been published by the authors who developed the software [3,9,10]. This paper aims at broadening the user community to foster progress in multiphase flow instabilities.

The software enables new research opportunities. To the best of our knowledge, no other open-source linear stability solver is capable of directly comparing the three Navier–Stokes models OB, LTD and FTD implemented. This enables, e.g., an assessment of the accuracy and the validity of the Oberbeck–Boussinesq approximation OB, which is an active research topic [11]. Moreover, the three interface models RI, SI and DI allow to study the role of dynamic interface deformations, which are often neglected. In ongoing work [6] regimes have been identified near the mechanical stability limit in which the flow-induced interface deformations have a significant impact on the basic state, hence on the stability of the system. The nonlinear temperature-dependence of the surface tension, implemented in DI, is important for large temperature differences. It allows users to investigate the effect of Marangoni stresses beyond the classic approximation SI.

`MaranStable` bears a great potential for significant extensions of its already advanced capabilities. Including evaporation and phase change would be of great interest. Moreover, including dynamic deformations caused by the perturbation flow would

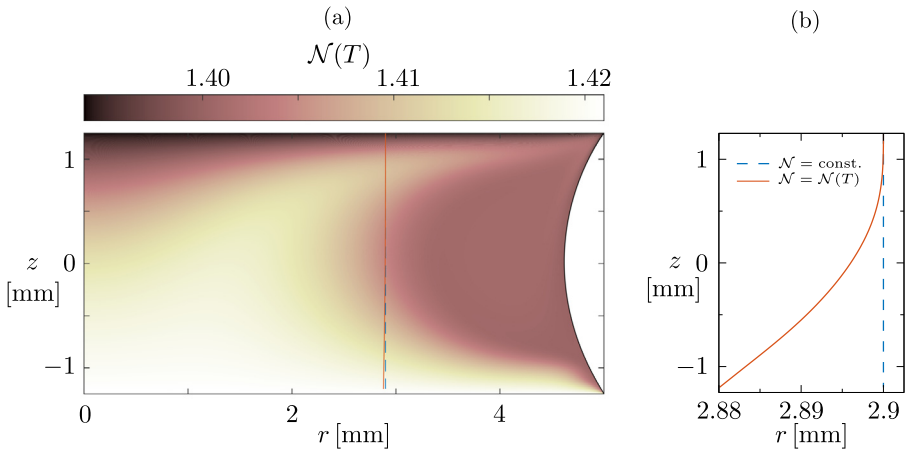

Fig. 5. Ray tracing in a non-isothermal liquid bridge: (a) Spatial distribution of the index of refraction $\mathcal{N}(T)$ [7] and optical path (red line) of a ray which enters or leaves the liquid perpendicular to the top (hot) transparent wall at $r = 2.9$ mm (blue dashes). (b) Close-up of the optical path.

allow the detection of surface wave instabilities. Adding the computation of the kinetic and thermal energy budgets of the critical mode to the post-processing tools would considerably support the physical understanding of the instabilities. Future extensions of `MaranStable` concern embedding implicit and explicit reduced-order models for heat transfer and wetting, including surfactant dynamics in the bulk and on the interface, and a generalization of the optical module.

Declaration of competing interest

The authors declare the following financial interests/personal relationships which may be considered as potential competing interests: Mario Stojanović reports financial support was provided by Austrian Research Promotion Agency. Hendrik C. Kuhlmann reports a relationship with Austrian Research Promotion Agency that includes: funding grants.

Data availability

Our data/code is available on https://github.com/fromano88/MaranStable.git.

Acknowledgments

This work has been supported by the Austrian Research Promotion Agency (FFG) in the framework of the ASAP14 programme under contract no. 866027. The first version of the `MaranStable` has been developed by Michael Lukasser in the framework of the project Engineering Marangoni Flows (EMA), which was also supported by FFG, Austria under contract no. 819714.

References

[1] Lehoucq RB, Sorensen DC, Yang C. ARPACK users' guide: Solution of large-scale eigenvalue problems with implicitly restarted Arnoldi methods. Philadelphia: SIAM; 1998.
[2] Gottlieb RG, Thompson BF. Bisected direct quadratic regula falsi. Appl Math Sci 2010;4:709–18.
[3] Stojanović M, Romanò F, Kuhlmann HC. Stability of thermocapillary flow in liquid bridges fully coupled to the gas phase. J Fluid Mech 2022;949:A5.
[4] Rayleigh, Lord. On convection currents in a horizontal layer of fluid, when the higher temperature is on the under side. Phil Mag 1916;32:529–46.
[5] Chandrasekhar S. Hydrodynamic and hydromagnetic stability. Oxford: Oxford University Press; 1961.
[6] Stojanović M, Romanò F, Kuhlmann HC. Flow instability of high-Prandtl-number liquid bridges accounting for the full temperature dependence of the thermo-physical properties (unpublished).
[7] He J, Liu W, Huang Y-X. Simultaneous determination of glass transition temperatures of several polymers. PLoS One 2016;11:1–12.
[8] Romanò F, Kuhlmann HC, Ishimura M, Ueno I. Limit cycles for the motion of finite-size particles in axisymmetric thermocapillary flows in liquid bridges. Phys Fluids 2017;29:093303.
[9] Stojanović M, Kuhlmann HC. Stability of thermocapillary flow in high-Prandtl-number liquid bridges exposed to a coaxial gas stream. Microgravity Sci Technol 2020;32:953–9.
[10] Stojanović M, Romanò F, Kuhlmann HC. Instability of axisymmetric flow in thermocapillary liquid bridges: Kinetic and thermal energy budgets for two-phase flow with temperature-dependent material properties. Eur J Appl Math [submitted for publication].
[11] Zonta F, Soldati A. Stably stratified wall-bounded turbulence. Appl Mech Rev 2018;70:040801.